1275140

THE UNITED STATES OF AMERICA

TO ALL TO WHOM THESE PRESENTS SHALL COME:

UNITED STATES DEPARTMENT OF COMMERCE

United States Patent and Trademark Office

January 19, 2005

THIS IS TO CERTIFY THAT ANNEXED HERETO IS A TRUE COPY FROM THE RECORDS OF THE UNITED STATES PATENT AND TRADEMARK OFFICE OF THOSE PAPERS OF THE BELOW IDENTIFIED PATENT APPLICATION THAT MET THE REQUIREMENTS TO BE GRANTED A FILING DATE.

APPLICATION NUMBER: ***60/527,455***
FILING DATE: ***December 05, 2003***
RELATED PCT APPLICATION NUMBER: ***PCT/US04/40298***

Certified by

Under Secretary of Commerce
for Intellectual Property
and Director of the United States
Patent and Trademark Office

Please type a plus sign (+) inside this box → [+]

PTO/SB/16 (10-01)
Approved for use through 10/31/2002. OMB 0651-0032
Patent and Trademark Office; U.S. DEPARTMENT OF COMMERCE
Under the Paperwork Reduction Act of 1995, no persons are required to respond to a collection of information unless it displays a valid OMB control number.

PROVISIONAL APPLICATION FOR PATENT COVER SHEET

This is a requ st f r filing a PROVISIONAL APPLICATION FOR PATENT under 37 CFR 1.53 (c).

22387 U.S.PTO
60/527455

Express Mail Label N . EV 092 038 490 US

INVENTOR(S)

Given Name (first and middle [if any])	Family Name or Surname	Residence (City and either State or Foreign Country)
Lin	Chia-Ying	Ann Arbor, Michigan
Scott	Hollister	Ann Arbor, Michigan

☐ *Additional inventors are being named on the _____ separately numbered sheets attached hereto*

TITLE OF THE INVENTION (280 characters max)

BIODEGRADABLE/BIORESORBABLE TISSUE AUGMENTATION/RECONSTRUCTION DEVICE

CORRESPONDENCE ADDRESS

Direct all correspondence to:

☒ Customer Number 27572

OR *Type Customer Number here*

☐ Firm *or* Individual Name	Harness, Dickey & Pierce, P.L.C.				
Address	P.O. Box 828				
Address					
City	Bloomfield Hills	State	MI	ZIP	48098
Country	USA	Telephone	248-641-1600	Fax	248-641-0270

ENCLOSED APPLICATION PARTS *(check all that apply)*

☒ Specification *Number of Pages* 29 ☐ CD(s), Number

☒ Drawing(s) *Number of Sheets* 8 ☒ Other (specify) Exhibit "A" (10 pgs); postcard

☒ Application Data Sheet. See 37 CFR 1.76 ☒ Specification Filed in English

METHOD OF PAYMENT OF FILING FEES FOR THIS PROVISIONAL APPLICATION FOR PATENT *(check one)*

☒ Applicant claims small entity status. See 37 CFR 1.27.

☒ A check or money order is enclosed to cover the filing fees

FILING FEE AMOUNT ($) $80.00

☐ The Commissioner is hereby authorized to charge filing fees or credit any overpayment to Deposit Account Number: 08-0750

☐ Payment by credit card. Form PTO-2038 is attached.

The invention was made by an agency of the United States Government or under a contract with an agency of the United States Government.

☐ No.

☒ Yes, the name of the U.S. Government agency and the Government contract number are: National Institute of Health - Grant Nos. DE13416, DE13608 .

Respectfully submitted,
SIGNATURE _____

TYPED or PRINTED NAME S.M. Erjavac / J.L. Snyder

TELEPHONE 248 641-1600

Date 12/05/03

REGISTRATION NO. (*if appropriate*) 38,442/43,141

Docket Number: 2115-002753

USE ONLY FOR FILING A PROVISIONAL APPLICATION FOR PATENT

PTO/SB/17 (01-03)
Approved for use through 10/31/2002. OMB 0651-0032
U.S. Patent and Trademark Office: U.S. DEPARTMENT OF COMMERCE

FEE TRANSMITTAL for FY 2004

Patent fees are subject to annual revision.

☒ Applicant claims small entity status. See 37 CFR 1.27

TOTAL AMOUNT OF PAYMENT ($) 80

Complete if Known	
Application Number	Unknown
Filing Date	Herewith
First Named Inventor	Lin Chia-Ying, et al.
Examiner Name	
Art Unit	
Attorney Docket No.	2115-002753

METHOD OF PAYMENT (check all that apply)

☒ Check ☐ Credit card ☐ Money Order ☐ Other ☐ None

☐ Deposit Account:

Deposit Account Number: 08-0750

Deposit Account Name: Harness, Dickey & Pierce, P.L.C.

The Director is authorized to: *(check all that apply)*
☐ Charge fee(s) indicated below ☒ Credit any overpayments
☒ Charge any additional fee(s) during the pendency of this application
☐ Charge fee(s) indicated below, **except for the filing fee** to the above-identified deposit account.

FEE CALCULATION

1. BASIC FILING FEE

Large Entity Fee Code	Large Entity Fee ($)	Small Entity Fee Code	Small Entity Fee ($)	Fee Description	Fee Paid
1001	770	2001	385	Utility filing fee	
1002	340	2002	170	Design filing fee	
1003	530	2003	265	Plant filing fee	
1004	770	2004	385	Reissue filing fee	
1005	160	2005	80	Provisional filing fee	80

SUBTOTAL (1) ($) 80

2. EXTRA CLAIM FEES

			Extra Claims		Fee from below		Fee Paid
Total Claims		-20 ** =	0	X		=	0
Independent Claims		-3 ** =	0	X		=	0
Multiple Dependent				X		=	0

Large Entity Fee Code	Large Entity Fee ($)	Small Entity Fee Code	Small Entity Fee ($)	Fee Description
1202	18	2202	9	Claims in excess of 20
1201	86	2201	43	Independent claims in excess of 3
1203	290	2203	145	Multiple dependent claim, if not paid
1204	86	2204	43	** Reissue independent claims over original patent
1205	18	2205	9	** Reissue claims in excess of 20 and over original patent

SUBTOTAL (2) ($) 0

**or number previously paid, if greater; For Reissues, see above

FEE CALCULATION (continued)

3. ADDITIONAL FEES

Large Entity Fee Code	Large Entity Fee ($)	Small Entity Fee Code	Small Entity Fee ($)	Fee Description	Fee Paid
1051	130	2051	65	Surcharge - late filing fee or oath	
1052	50	2052	25	Surcharge - late provisional filing fee or cover sheet.	
1053	130	1053	130	Non-English specification	
1812	2,520	1812	2,520	For filing a request for reexamination	
1804	920*	1804	920*	Requesting publication of SIR prior to Examiner action	
1805	1,840*	1805	1,840*	Requesting publication of SIR after Examiner action	
1251	110	2251	55	Extension for reply within first month	
1252	420	2252	210	Extension for reply within second month	
1253	950	2253	475	Extension for reply within third month	
1254	1,480	2254	740	Extension for reply within fourth month	
1255	2,010	2255	1,005	Extension for reply within fifth month	
1401	330	2401	165	Notice of Appeal	
1402	330	2402	165	Filing a brief in support of an appeal	
1403	290	2403	145	Request for oral hearing	
1451	1,510	1451	1,510	Petition to Institute a public use proceeding	
1452	110	2452	55	Petition to revive – unavoidable	
1453	1,330	2453	665	Petition to revive – unintentional	
1501	1,330	2501	665	Utility issue fee (or reissue)	
1502	480	2502	240	Design issue fee	
1503	640	2503	320	Plant issue fee	
1460	130	1460	130	Petitions to the Commissioner	
1807	50	1807	50	Processing fee under 37 CFR 1.17 (q)	
1806	180	1806	180	Submission of Information Disclosure Stmt	
8021	40	8021	40	Recording each patent assignment per property (times number of properties)	
1809	770	2809	385	Filing a submission after final rejection (37 CFR § 1.129(a))	
1810	770	2810	385	For each additional invention to be examined (37 CFR § 1.129(b))	
1801	770	2801	385	Request for Continued Examination (RCE)	
1802	900	1802	900	Request for expedited examination of a design application	

Other fee (specify) _____

*Reduced by Basic Filing Fee Paid

SUBTOTAL (3) ($) 0

SUBMITTED BY

Complete *(if applicable)*

Name (Print/Type)	S.M. Erjavac/J.L. Snyder	*Registration No. Attorney/Agent)*	38,442/43,141	*Telephone*	248 641-1600
Signature	Jeffrey L. Snyder			*Date*	December 5, 2003

WARNING: Information on this form may become public. Credit card information should not be included on this form. Provide credit card information and authorization on PTO-2038.

BIODEGRADABLE/BIORESORBABLE TISSUE AUGMENTATION/RECONSTRUCTION DEVICE

GOVERNMENT RIGHTS

[0001] This invention was made with government support under Grant Nos. DE13416, DE13608 awarded by the National Institute of Health. The Government may have certain rights in the invention.

FIELD OF THE INVENTION

[0002] The present invention relates to biodegradable materials and, more particularly, relates to a method of optimizing the design of biodegradable materials.

BACKGROUND AND SUMMARY OF THE INVENTION

[0003] There is growing interest in using biodegradable materials to replace permanent materials for many reconstruction applications. Degradable materials, however, are less stiff than permanent materials and suffer further stiffness reduction through time. Merely replacing the permanent material with a degradable material in the same design may lead to early device failure. Since many degradable materials lose material through bulk erosion without shape change, we hypothesize that a topology optimization method accounting for base material degradation could create a degradable device that retains sufficient stiffness through the degradation process. The proposed optimization method creates a density distribution map for selected time points during degradation.

These different density distributions are then linearly superposed using both time and degraded base stiffness weighting factors. In this paper, the method is applied to design a degradable spinal fusion cage device from poly(propylene fumarate)/beta-tricalcium phosphate (PPF/β-TCP).

[0004] Further areas of applicability of the present invention will become apparent from the detailed description provided hereinafter. It should be understood that the detailed description and specific examples, while indicating the preferred embodiment of the invention, are intended for purposes of illustration only and are not intended to limit the scope of the invention.

DETAILED DESCRIPTION OF THE PREFERRED EMBODIMENTS

[0005] The following description of the preferred embodiment(s) is merely exemplary in nature and is in no way intended to limit the invention, its application, or uses.

I. Current trends and design types of biodegradable/bioresorbable tissue augmentation/reconstruction devices

[0006] The use of biodegradable material for tissue augmentation/reconstructions devices has become increasing prevalent to facilitate tissue regeneration and improve integration with host tissues. The concept extended from previous laboratory-scale scaffold implantations to current focuses on the application of devices such as cartilage repair units, rotator cuff anchors, intravascular stents, bone screws and plates made with poly(DL-lactic acid) or poly(L-lactic acid) (Figure 1a, 1b, and 1c). However,

simply replacing the base material from the original design with biodegradable polymers may not be appropriate, especially for the development of load bearing devices in joint reconstructions and spine arthrodeses since degradable materials typically have less stiffness and strength than non-degradable materials. Furthermore, this stiffness and strength will degrade over time, further reducing the mechanical competency of the device. The goal is to retain adequate stiffness and strength until tissue regeneration is sufficient for the tissue to assume load bearing function.

[0007] Implants should be designed to provide sufficient stiffness for tissue regeneration and reunion to occur before degradation. A prime example of the importance of device stiffness is spinal fusion cage design. Conventional designs of the spinal interbody fusion cages have mainly focused on providing immediate strength to maintain disc height and shielding the bone grafts within the cage. Therefore, the geometrical features of these conventional designs show little distinction from each other and most of them fall into a category of a pipe shape with thick shells as outer walls as well as a hollow interior space that brackets the fill of grafting materials (Figure 2). Further division is defined by the threaded and non-threaded anchorage mechanism that cage devices rely on to form rigid bonds with vertebral bodies. Threaded designs may be utilized along the entirely outer surface for cylindrical cages, whereas they are distributed only on two collateral sides perpendicular to the insertion plane and later wedged into the endplates of the vertebral bodies (Figure 3). These hollow pipe designs guarantee sufficient reconstruction stiffness in arthrodesis and play a substantial

role in stability for motion segments postoperatively. However, this concept will not remain true once degradable polymers replace metallic materials in the same design. The original designed architectures will only perform as they are proposed when these devices are made with permanent materials such as metallic alloys.

[0008] Another major concern for using metallic implants is that the enormously high magnitude of the stiffness compared to bone tissue may shield an implanted graft or ingrown bone tissue from sufficient mechanical stimulus, (known as "stress-shielding") thus increasing the risk for decreased mineralization and bone resorption. This effect is seen in hip joint arthroplasties where significant bone loss around the hip stem is seen due to stress shielding. Long-term follow-up of the lumbar spine arthrodesis also indicates decreased mineralization inside the cage due to stress shielding.

[0009] Recently, poly(alpha-hydroxy esters) have been investigated as resorbable interbody fusion cages (Figure 4 and 5). Base material replacement without changing cage design demonstrated that reduced stiffness of the resorbable cages significantly improved fusion compared to the titanium cage when implanted in sheep. However, there is still concern that degradable spine cages will lack sufficient load bearing capability, especially given the fact that cages will lose stiffness and strength over time. In addition, loads in the human spine are much higher than in sheep spine. Because the base material stiffness will undergo persistent reduction through the degradation, merely replacing a

non-degradable material with a degradable material in the same design may not produce a device that retains sufficient load bearing capability.

[0010] In the present invention, the method of integrated topology optimization incorporated with weighing factor design is proposed to ensure that biodegradable devices have sufficient mechanical properties initially and during degradation. Prolonging stiffness through the degradation was achieved by weighting material density to compensate for reduced base material stiffness and lost structural features caused by the bulk erosion.

II. New design approach of the invention to define reinforced global material distribution

[0011] There are two types of degradation mechanisms for biodegradable materials: 1) bulk erosion and 2) surface erosion. Many commonly used degradable polymers including polylactic acid, polyglycolic acid, and poly(propylene) fumarate, undergo bulk erosion. Bulk erosion under the hydrolysis mechanism in physiological environments will not dramatically change the conformation but will decrease the molecular weight gradually during the degradation process. Therefore, the strength and stiffness decays even though the shape and volume do not change significantly. Based on the phenomenon, the approach that tends to utilize the structural reinforcement will have minor contributions to the entire integrity especially at the later stage of the degradation.

[0012] Our goal of the invention is to design biodegradable/bioresorbable tissue augmentation/reconstruction devices such that these devices fulfill the multiple requirements of initial mechanical support, scaffolding for vascular supply and ingrown tissue, porous architecture for biofactor delivery as well as the sufficient residual stiffness through the degradation process to form new constructs with growing tissues. Therefore, a specific design approach will be required for degradable devices such that the stiffness satisfies load bearing requirements at time 0. Sufficient stiffness must also be maintained through degradation until devices are fully integrated with or replaced by new tissue. This design technique will allow better control of material mechanical properties during the degradation process to better match the increasing mechanical properties of regenerating tissue.

[0013] Spinal fusion cages are a prime example of a device that needs to meet multiple requirements for load bearing and tissue regeneration. A suitable design for spine interbody fusion cages needs to limit displacements for stability, allow sufficient strain energy density transfer to ingrown bone to reduce stress shielding, and achieve desired porosity for tissue ingrowth. These objectives must even be met at each time during the degradation process when adopting degradable materials. The replacement of current permanent materials such as metals or carbon fibers with the degradable polymer reduces the stress shielding environment, but the higher compliance of degradable materials coupled with the continual stiffness reduction due to degradation will lead to insufficient load bearing capabilities if no compensation mechanism is

incorporated in the initial design. Therefore, the design for a biodegradable spine interbody fusion cage should also take into account the maintenance of sufficient load bearings through the degradation.

[0014] In this invention, we propose a new approach for biodegradable devices by using integrated local/global topology optimization that incorporates the degradation profile of the degradable material. In topology optimization, the design is discretized into finite elements, and each element will contain a predicted material density between 0 and 1. In the degradation design, the density in each element is weighted by the degradation profile. By altering the material weights in each element by applying two weighting factors, the weighted material density in each element within the global optimized topology will compensate the loss of the degraded material from the original designs and retain sufficient stiffness through the degradation process. The two weighting factors are 1) time lasting factor: defined as (total degradation period - time of selective point)/total degradation period. This factor accounts for the influence of the time past implantation on reinforcement of the scaffold architecture. 2) degrading modulus factor: defined as reduced modulus at the selected time divided by the original modulus. The factor indicates the weight percentage of the original material equivalent to the superposed material densities based on the degrading modulus at selected time points. The two factors have been introduced according to the lasting time of the degrading material and the reduced base stiffness of the material at selected time points during the degradation process. These two factors together can utilize the superposed

material for the reinforcement in a more efficient manner since they take both the degree of modulus reduction and the time past implantation into account. As time proceeds further past implantation, tissue ingrowth will begin to carry load, reducing the need for scaffold structure. The weighted material distribution can reinforce the stiffness at the regions that require denser material to provide sufficient load bearing especially when the base material stiffness is reduced due to the bulk erosion. Thus, the weighting process produces designs where high load bearing regions are reinforced to compensate for subsequent stiffness degradation due to bulk erosion.

[0015] For biodegradable/bioresorbable tissue augmentation/ reconstruction devices, the design should balance requirements of sufficient stability, compliance to avoid stress shielding and porosity for biofactor delivery. In addition, sufficient stiffness must also be maintained through degradation until devices are fully integrated with or replaced by new tissue. Requirements of stability, reduced stress shielding, and porosity for biofactor delivery together with the need to balance these requirements through the degradation period present a number of conflicting design alternatives. Stability requires a denser material while compliance and biofactor delivery require greater porosity. Achieving a balanced design requires an optimization approach. Specifically, we desire to create a material layout such that stability, compliance and porosity requirements can be optimally balanced while at the same time accounting for material degradation. We have utilized a unique two scale topology optimization approach to create the optimal material layout for desired stability, compliance and

porosity. The macroscopic or 1st scale topology optimization solution provides the general density and location of material within the implant site to limit the displacement under applied load for desired stability with a constraint to enforce the desired porosity. The microscopic or 2nd scale topology optimization approach gives the specific microstructure design that achieves a desired compliance while matching the predicted volume fraction of the macroscopic or 1st level topology optimization.

[0016] To meet the objectives mentioned above for biodegradable/bioresorbable tissue augmentation/reconstruction devices, the macroscopic or 1st scale topology optimization is used to design the material layout for selected time steps during the degradation process. The design domain for any biodegradable/bioresorbable tissue augmentation/reconstruction device can be defined with arbitrary shapes according to the implant size, anatomic geometry, and/or disease/injury requirement. The optimal material distribution through out the entire design domain is computed using topology optimization. The effective modulus is interpreted by the density method as Eijkl=XpEijkl0 to indicate the solid, porous and void regions, where Eijkl represents the effective modulus of each finite element, Xp is the fraction of the material and the base material property is Eijkl0. This weighting method is used since a degrading material must have greater density at time 0 than an equally stiff non-degrading material to retain stiffness post-implantation that meets desired design objectives. Therefore, the optimal density distribution for the degradable device material is created by superposing the multiple time optimal

densities weighted by a time lasting factor Twt = (Ttotal – Tcurrent)/Ttotal and degrading modulus factor Ewt = Et/E0 as Xpw=Σ XptTwtEwt, where Xpw is the final fraction of the base material, Xpt is the temporary fraction of the reduced/degraded modulus corresponding to a selected time point, and Twt, Ew are time lasting factor and degrading modulus factor for selected time points as mentioned and defined previously.

[0017] The example of a biodegradable spine interbody fusion cage design using poly(propylene fumarate)/beta tricalcium phosphate demonstrates how the disclosed approach was applied to develop a device that meets critical requirements and objectives concurrently through the degradation. A global topology optimization algorithm (Optistruct, Altair Computing, Inc.) was used to predict a global layout density under the constraint that strain at the vertebral surface were less than 8%. Two rectangular blocks as the designable components were established to represent the location of the implanted cages and the multi-directional loads of the physiological range including compression, lateral bending, torsion, and flexion-extension were applied to the constructed segment. A finite element model was then created to simulate the mechanical environment of the design domain within the disc space (Figure 6). The optimal design of the cage topology is interpreted by block configurations of elements corresponding to the respective material density between 0 to 1 where 0 indicates void space and 1 indicates total solid element; values in between indicate corresponding material volume fraction that occupies the element space. At the selected time points through the degradation, denser topological

arrangement of the material forms to reflect that more material should be placed in the structure to maintain sufficient stiffness that is gradually reduced due to the degrading base material by bulk erosion (Figure 7). Namely, the longer time the degradable device will go through, the higher the density of the material needed initially to compensate for the degrading stiffness to maintain adequate load bearing. However, the required higher material density at the selected time will only need to be satisfied for the time period from the beginning of the selected time until the end of the degradation. Therefore, the reinforcement design is flexible to match the needed time duration, avoiding excess use of material for long degradation periods.

[0018] Figures 7a to 7d represent show that the reduced base material stiffness generated denser material distribution through the degradation compared to the initial topology with the original base material. The red indicates higher density and becomes more prevalent at later time stages as the design becomes denser to account for a reduced base material stiffness. This suggests that for biodegradable devices, it is inappropriate to design the whole architecture merely based on the initial properties as the design for devices with permanent materials. Rather, certain reinforcements should be incorporated to compensate for degrading stiffness in higher loaded regions. Weighting material densities are applied to determine the location of higher density structural reinforced regions during degradation. Figures 7a to 7d show the required material distributions for $t = 0T$, $0.5T$, $0.55T$, $0.85T$ (T: degradation duration), with the effective compressive moduli of E, 0.875E, 0.78E, 0.25E, respectively. The final density

of each element thus should be expressed as: $Xpw=\Sigma XptTwtEwt$, where Xpt is the temporary density level based on reduced/degraded modulus at selected time points, Ewt is the percentage of the original modulus accounting for the degraded material at the selected time point, and Xpw in this case is the final density which is equal to $Xp1+Xp2\times0.5\times0.875+ Xp2\times0.5\times0.875+ Xp3\times0.45\times0.78+ Xp4\times0.15\times0.25$.

III. Microstructures as periodic unit cells in material constitution

A. Introduction of microstructure design

[0019] A drawback of the general structural layout is that it creates transitional densities other than 0 or 1. This numerical difficulty could imply that current mesh resolution cannot carry out the structure to achieve the objective function, and has been addressed as a mesh dependent problem. Different numerical techniques such as penalty schemes have been used to impel the element density to 1 or 0 under artificial material laws, which represent the element with solid (base material) or void (no material). From a material science point of view, we can instead view the intermediate density values from the global topology optimization as representing a microstructure defined at a different length scale than the global optimization. The microstructure of composite material could be categorized into different rank, defined by different length scales, and the microstructure of particular rank will be homogenized for its upper rank (Figure 8). This physical phenomenon allows us to propose a new approach to deal with elements of intermediate density by introducing an

additional rank of material design for the particular element. Instead of choosing element of global design between 1 and 0, we can now obtain microstructures from the base material that can represent those elements with ambiguous intermediate densities as shown in Figure 9. In other words, we will assume that densities between 0 and 1 can be replaced with a different scale of microstructure. This microstructure will be designed using microstructure or local topology optimization techniques.

[0020] Designing materials microstructure allows creation of structures with an extremely wide range of elastic properties. For example, materials with negative Poisson's ratio (NPR), which expands transversely when subject to an applied tensile load, can be used in many applications such as fasteners and shock observers. Furthermore, in the sense of "design", one may create the material with prescribed and specified value of material properties, such as elasticity, permeability, and dynamic performance, for a specialized application within the physical manner. For the implementation of material microstructure design for elasticity, homogenization theory with periodic boundary conditions (PBC) will be used for the design domain. Moreover, in order to theoretically calculate the effective properties of material with periodic microstructure pattern, A Finite-Element based homogenization technique is utilized, (Hollister, S., J. Brennan, and N. Kikuchi, A Homogenization Sampling Procedure for Calculating Trabecular Bone Effective Stiffness and Tissue Level Stress. J. of Biomechanics, 1994. 27(4): p. 433), with the weak form of the equilibrium constitutive equation is

solved numerically using Element-By-Element Preconditioning Conjugate Gradient (EBE-PCG) to obtain the effective elastic properties.

[0021] Two optimization algorithms, denoted as full topology optimization and restricted topology optimization, are introduced to perform the microstructural level design, as described in the following sections.

B. Full Topology Optimization: Microstructure Design De Novo to achieve elastic properties

[0022] Design material microstructure using Topology Optimization was first implemented by Sigmund, O. in 1997, and the problem can be considered as an optimal material distribution problem within the periodic design domain and solved using Sequential Linear Programming (SLP) optimization technique. A generalized optimization problem formulation can be stated as (1).

$$\min_X \; w_1 \left\| C_1^H - C_1^* \right\|_{L_2} + w_2 \left\| C_2^H - C_2^* \right\|_{L_2} + \ldots.$$

s.t.

$$C_3^H \geq C_3^*$$

Volume fraction constraints on the constituent base material.....(1)

Symmetric of design domain constraints

Connectivity of structure constraints

Bounds on design variables

[0023] C could be any material properties to be designed by minimizing the L2 norm of difference between effective properties with target properties. wi are weighting parameters. This nonlinear optimization is now solved using Method of Moving Asymptotes (MMA), which was developed Svanberg in 1987. The current approach in literature, however, suffers from numerical difficulties

when implement in the 3 dimensional case. We have made two significant algorithmic enhancements to address these numerical difficulties associated with full topology microstructure design. The first crucial technique was developed to deal with the design dependency of initial guess, and convergence improvement. Because of the periodic boundary condition, the optimal result is not unique (Figure 10) and depends significantly on the initial guess of the design process. To address this issue, a low resolution mesh with homogeneous density is used first as an initial guess in the optimization process. This problem is then solved, and the resulting solution is meshed at a much finer resolution and used as an initial guess for the next set of iterations. The process ends when the best resolution is reached and converged. The detail design procedure can be illustrated in flow chart (Figure 11).

[0024] The second enhancement involves application of image processing techniques during the topology optimization in order to eliminate checkerboard density pattern. The element density is smoothed with surrounding elements using a Gaussian smoothing filter and also a connectivity filter within each optimization iteration. After elimination of checkerboarding, or rapid fluctuation in density over short scales, the final microstructure design will still have transitional density ranging between 0 and 1, and to minimize the impact of final filtering, a heuristic based random rounding technique is developed. From the idea of integer programming, the density distribution in the design domain can also be considered as probability distribution for discrete optimization, hence we will have infinite final design generate from the probability table and the best

one that satisfy all the design criteria will be chosen to become the optimal microstructure layout.

C. Restricted Topology Optimization: Microstructure Design assuming a priori topology to achieve elastic properties Alternative microstructure options-size optimization (restriction design)

[0025] Another approach to define the microstructure of the periodic unit cell is to assume an initial topology with a restricted number of design variables describing the topology. For example, one possible design is that of interconnecting cylindrical pores, where the design variables are the pore diameters (Figure 12). In this approach, stiffness was chosen to represent scaffold function and porosity represented the scaffold's capability to enhance tissue regeneration. This can be further divided into two design options: if the primary goal is to design a scaffold such that the scaffold itself and regenerate tissue match desired mechanical properties while maintaining a base level of porosity, the optimal design problem, denoted as the stiffness design, can be written as

Objective function:

$$\underset{E^{scaffold},\, d_1,\, d_2,\, d_3}{\text{Min}} \left\{ \sum_{i=1}^{n} \left(\frac{C_i^{\text{bone eff}} - C_i^{\text{tissue eff}}}{C_i^{\text{bone eff}}} \right)^2 + \sum_{i=1}^{n} \left(\frac{C_i^{\text{bone eff}} - C_i^{\text{scaffold eff}}}{C_i^{\text{bone eff}}} \right)^2 \right\},$$

where $n = 1-9$.

Constraints:

$$d_1,\ d_2,\ d_3 \leqslant 900\ \mu\text{m},$$

$$d_1,\ d_2,\ d_3 \geqslant 300\ \mu\text{m},$$

$$\frac{V_{\text{pore}}}{V_{\text{total}}} \geqslant \%\text{Porosity},$$

$$E^{\text{scaffold}} \geqslant E_{\min},$$

$$E^{\text{scaffold}} \leqslant E_{\max},$$

where design variables include $E^{scaffold}$, the scaffold base material Young's modulus and d1,d2, and d3, the three cylinder diameters. $C^{bone\ eff}$ is the effective stiffness of the target bone, $C^{tissue\ eff}$ is the regenerate tissue effective stiffness, $C^{scaffold\ eff}$ is the scaffold effective stiffness. Thus the approach generates the structural interpretation consisting of three cylindrical chambers with computed diameters and the design modulus of corresponding configuration.

[0026] Instead, if the purpose of the design is to preserve large porosity for vascularization, plus both scaffold and regenerate tissue stiffness are maintained within an acceptable range, then the optimization problem denoted as the porosity design can be written as

Objective function:

$$\underset{E^{\text{scaffold}}, d_1, d_2, d_3}{\text{Max}} \frac{V_{\text{pore}}}{V_{\text{total}}}.$$

Constraints:

$$\alpha_1 C_i^{\text{bone eff}} \leqslant C_i^{\text{tissue eff}} \leqslant \alpha_2 C_i^{\text{bone eff}}$$
where $i = 1-9$; $\alpha_2 > \alpha_1$,
$$\beta_1 C_i^{\text{bone eff}} \leqslant C_i^{\text{scaffold eff}} \leqslant \beta_2 C_i^{\text{bone eff}}$$
where $i = 1-9$; $\beta_2 > \beta_1$,
$d_1,\ d_2,\ d_3 \leqslant 900\ \mu\text{m}$,
$d_1,\ d_2,\ d_3 \geqslant 300\ \mu\text{m}$,
$E^{\text{scaffold}} \geqslant E_{\min}$,
$E^{\text{scaffold}} \leqslant E_{\max}$,

where α1, α2,β1, and β2 are a scaling factors used to bound the scaffold and regenerate tissue effective stiffness and the variables are as defined above. Again, the computed design variable defines the final topology of the interconnecting channels by three cylindrical chambers with three diameters in the periodic unit cell shown in Figure 13.

D. Designed architectures to interpret ambiguous density distributions in global topology degradation optimized designs

[0027] Once we have the ability to design material microstructure for specified properties, we can deal with the transitional density range from the global topology optimization result. For this special spinal cage design case, we shall considered elasticity properties of materials. The upper bound and lower bound of elasticity of composite material were obtained theoretically, which

means for a particular volume fraction (or porosity), there is an upper bound and lower bound of stiffness an isotropic composite can achieve, or for a particular elasticity property, there is an upper bound and lower bound of composite volume fraction to achieve, as illustrated in Figure 14. This provides us two alternative ways to interpret the global topology density prediction. For instance, assume we have a global element with 0.5 density value (1) First, the element can be interpreted to have a unique microstructure with 50% volume fraction and the objective material properties for microstructure design could be the upper or lower Hashin-Shtrikman bound depending on whether the global structure design should to have extreme stiffness or compliance properties for that particular element. (2) Second, an alternative interpretation is that considered the element could have specified anisotropic effective properties, and the microstructure is designed is to achieved these particular properties with the smallest or largest volume fraction.

E. Defined interconnected channels with carriers for biofactor delivery

[0028] The microstructure design generates the interconnecting network of channels that define the biofactor delivery domain. The biofactors could include cell, genes, proteins or any combination of the three. The carriers could include hydrogels or polymers cast into these channels to release viable progenitor cells, genes or growth factors to achieve local bone tissue formation. Interconnecting channels can also provide favorable environments for

vascularization as they provide conduits for angiogenesis and mass transportation to maintain functions of new-forming tissues. Channels confined by surrounding microstructures also imply that the ingrowth bone can receive direct mechanical stimulation transferred by struts of these microstructures, reducing stress shielding.

IV. Integration of global layout and local microstructure optimal topology

[0029] The integrated global and microstructure topology optimization approach is used to define the final architecture of biodegradable/bioresorbable tissue augmentation/reconstruction devices that meets design requirements of sufficient stability, compliance to avoid stress shielding and porosity for biofactor delivery, while the sufficient stiffness is also maintained through degradation until devices are fully integrated with or replaced by new tissue. The global topology optimization algorithm is used to generate global density distribution under physiologic loading. Immediate stability is addressed by constraining the total displacement at the implant sites to be less than a desired target. Total porosity for biofactor delivery and sufficient compliance to avoid stress shielding is input as a constraint for the global optimization at each selected time point through the degradation. The result is a global volume fraction distribution that also considers the reinforcement for the stiffness reduced through degradation by linearly superposing different density distributions at selected time points using both time and degraded base stiffness weighting factors. The layout density threshold was then processed to segment the entire interconnected architecture

to four separate material phases of complete solid, high percentage solid, low percentage solid, and completely void (0% material) regions to match the target porosities of the microstructure design while maintaining sufficient stiffness and acceptable connectivity. Note that the global material layout only provides a porosity and does not define the topology of the porous microstructure. To further define the microstructure, a local microstructural topology optimization method was used to generate periodic microstructures for the high percentage and low percentage solid regions that achieved Hashin-Shtrikman stiffness bounds for porous isotropic materials. The entire device design could then be generated by alternating periodic microstructures within the global density layout. The density of the global layout served as a flag to assign the microstructural topology. The overall volume fraction was closely held at that of the original global layout optimal topology after the replacement of original global elements with designed microstructures. The resulting porous cage architecture can also serve a dual purpose as a delivery vehicle that would be appropriate for therapeutic cell transplantation.

[0030] A schematic flow chart of the design process can be seen in FIG. 19. For further description of the present invention, please refer to attached Exhibit A, which is provided originally in color.

V. Results

[0031] Our prototype demonstrates an example of applying our proposed design methodology for biodegradable devices to spine interbody

fusion cage design. The cage design domain was constructed with 8 by 5 by 4 elements, the size of which is exactly the same as the microstructure dimension. The base material for the example is a biodegradable polymer composite of poly(propylene fumarate)/β-tricalcium phosphate) (PPF/β-TCP). A composite material of poly(propylene fumarate)/beta-tricalcium phosphate was selected as the exemplary biodegradable polymer since it has been proved to be osteoconductive and upon degradation yields primarily fumaric acid and propylene glycol that can be removed by normal metabolic pathways. Optimal topology for each selected time points was represented in density distribution in block configuration as shown in Figure 15. Note that it is reasonable that the structure designed for degradation will be denser than other structures as the added material is needed to compensate for the reduced stiffness over time. The layout density threshold was processed to segment the entire interconnected architecture to four separate material phases of 100% solid, 55% solid, 35% solid, and completely void (0% material) so that the layout of each layer is composed of three values of grayscale referred to the corresponding regions. Figure 16(a) shows the segmentation process on the initial density distribution at time 0 without applying the material density weighting. When applying the material density weighting with consequent material density distributions of reduced base material stiffness, certain regions were reinforced with weighted material density shown in the segmented layout as in Figure 16(b). The local microstructural topology optimization method then generated periodic microstructures for the 55% and 35% solid regions (Figure 17).

[0032] The prototype of the designed cage was achieved by automatically converting the image-design data to a surface representation in .STL format. The image-design data was also converted to contour .SLF format. The .STL and contour was then loaded in 3-D printing machine for the preparation of wax molds. Poly(propylene fumarate) (Mn = 1200) cross-linked by N-vinyl pyrrolidone combined with beta-tricalcium phosphate (PPF/β-TCP) was cast in the prepared molds. Final prototypes are shown below in Figure 18 for both designs with and without the material weighting.. The actual size for the prototype is 24 mm x 15mm x 12 mm, with 5 and 4 microstructures making up the cross-sectional areas and 8 on long one.

[0033] The degradation characterization experiment to verify the invention has been conducted for three cage designs fabricated (N=24 per design) with poly(propylene fumarate) cross-linked by N-vinyl pyrrolidone combined with beta-tricalcium phosphate. These designs included a standard threaded cage (standard: CONCAGE), a cage optimized for initial properties (optimized: OSCAGE), and a cage optimized accounting for degradation (degrading optimized: OSCAGEDEG). Samples from each group underwent degradation under the conditions described in the ISO13781 standard. Micro-CT scanning, mechanical testing, and weigh loss measurement were conducted to investigate the degrading properties at 0, 3, 6, and 12 weeks.

[0034] All cage designs decreased in material volume and weight while increasing in density after 3 weeks of degradation. The peak load and stiffness at time=0 and 3 weeks are shown in Table 1. Both structural properties remained

constant for CONCAGE, decreased during degradation for OSCAGE, and increased for OSCAGEDEG designs. The comparison of average material density change, ΔD%, volume fraction variation ΔV%, and weight change percentage ΔW% before and after 3 weeks of degradation are shown in Table 2. All cage designs decreased in material volume and weight while increasing in density after 3 weeks of degradation. However, the OSCAGEDEG design exhibited the greatest increase in density, lowest decrease in volume, coupled with actual improvement in mechanical properties after three weeks of degradation. Consecutive micro-CT scanning till 6 weeks showed slight geometrical change indicating bulk erosion without significant feature damage. The structural reinforcement of the degrading optimized design retained sufficient stiffness compared to the other two designs with significant dropping stiffness through the degradation.

Table 1	Peak Load (N)		Stiffness (N/mm)	
	0 wk	3 wk	0 wk	3 wk
CONCAGE	151±18	150±42	258±68	233±36
OSCAGE	842±107	427±17	1655±428	925±121
OSCAGEDEG	1259±382	1659±81	1723±560	3262±391

Table 2	ΔD%	ΔV %	ΔW %
CONCAGE	9.4±7.6	-1.1±0.69	-16.17±0.26
OSCAGE	5.8±2.1	-0.93±0.36	-20.95±0.49
OSCAGEDEG	15.1±12.1	-0.34±0.10	-17.90±1.07

[0035] Increased stiffness in OSCAGEDEG suggests the weighted density reinforced the degraded structure. CONCAGE maintained integrity after 3 weeks, whereas the stiffness of OSCAGE decreased in integrity. In all groups, an increase of material density may cause an increase in bulk properties of the material. This result may be consistent with previous studies that show an increase in crosslinking density of PPF/β-TCP composite after 3 weeks. The OSCAGEDEG design showed the least volume fraction variation, indicating the weighted density may resist bulk erosion. Meanwhile, the weighting that contributed to primary load bearing significantly increased the stiffness (4x increase) compared to OSCAGE design with only 10% volume fraction increase after the weighting. The effective stiffness was even higher than CONCAGE (8x increase). This study demonstrated a potential to utilize the weighted optimal density as a feasible approach to design biodegradable cages or other orthopedic devices.

VI. Conclusion

[0036] Currently, biodegradable polymers have offered researchers and scientists a possible solution to the waste-disposal problems associated with

traditional petroleum-derived plastics. Innovative new biomedical applications, including artificial skin, heart valves, and other organs grown on biopolymer scaffolding, are creating major opportunities for new product development and the commercial exploitation of these materials.

[0037] Biopolymers, which can be either derived from natural or synthetic materials, provides a number of advantages over traditional synthetic plastics derived from petroleum. They are biodegradable/bioabsorbable, and therefore environmentally friendly, as well as biocompatible, which makes them a suitable alternative to compounds such as silicone in medical applications. In addition to the development of biopolymer-based processes for growing artificial organs, scientists have successfully used biopolymers to create "drugs" that never enter the bloodstream, antibacterial coatings for medical devices, a microsponge technology that releases medical ingredients slowly over time, a collagen plug that revolutionizes postoperative care, and therapies based on hyaluranon, a specially tailored visco-elastic biopolymer.

[0038] The disclosed invention offers a new approach to give biopolymeric medical devices adequate mechanical performance for a variety of purposes. Biodegradable skin grafts need to provide stretch resistance before the full integration with the host parenchymal tissues, before then the reinforced material should be applied to prolong the structural integrity. Devices used to fix traumatic fractures require sustaining ultimate strength until the acceptable union occurs, but this is not easy to be achieved when utilizing biodegradable polymers. Implants for those sites with main load bearings especially need the

specific designed architecture to maintain the biomechanical functions. Thus, the invention provides a general design approach to fulfill individual demand of mechanical performances for each biodegradable/bioresorbable tissue augmentation/reconstruction device.

[0039] The description of the invention is merely exemplary in nature and, thus, variations that do not depart from the gist of the invention are intended to be within the scope of the invention. Such variations are not to be regarded as a departure from the spirit and scope of the invention.

CLAIMS

What is claimed is:

1. A method of designing a biodegradable/bioresorbable tissue augmentation/reconstruction implant, said method comprising:

employing a topology optimization algorithms to define material density distributions at selected time points during degradation; and

superposing said material density distribution using both time and degraded base stiffness weighting factors.

ABSTRACT OF THE DISCLOSURE

A new design approach for biodegradable/bioresorbable tissue augmentation/reconstruction implants has been developed by using topology optimization algorithms to define material density distributions at selected time points during degradation. These different density distributions are then superposed using both time and degraded base stiffness weighting factors. A topology optimization method accounting for base material degradation could create a degradable device that retains sufficient stiffness through the degradation process. Thus, any bulk degrading material can be designed using this process for any tissue augmentation/reconstruction application.

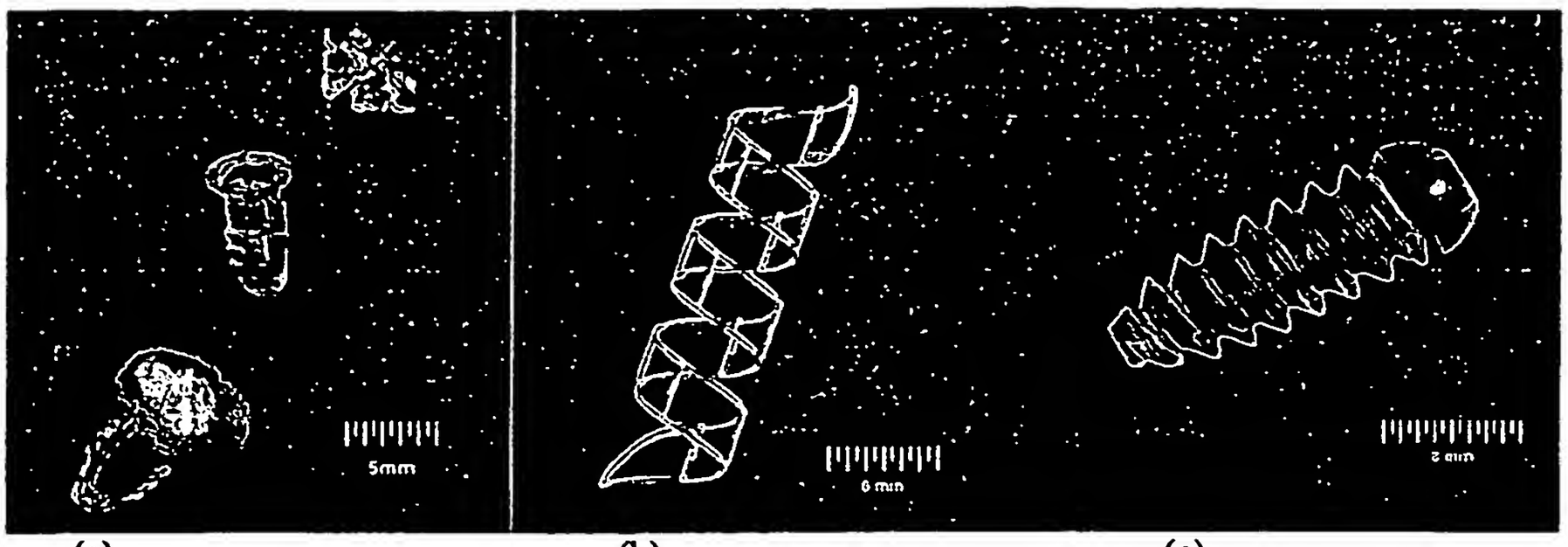

(a) (b) (c)

Figure 1: Various applications of bioabsorbable tissue augmentation/reconstruction devices and implants. (a) "ACRU/ACRS" cartilage repair unit, Matrix Biotechnologies, Inc. (b) Hybrid PLA/TMC intravascular stent prototype, Corids, Miami, FL (c) PLA 8mm Bio-Interference Screw, TESco Associates, Inc. (http://www.tescoassociates.com)

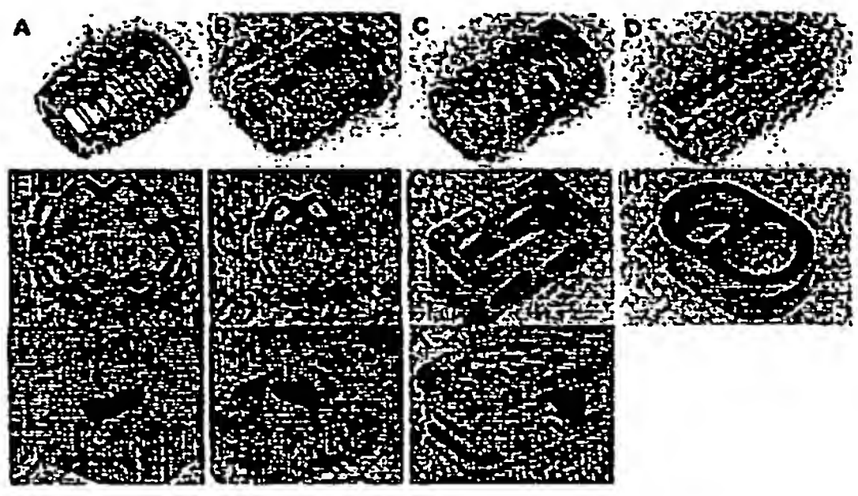

Figure 2 Interbody fusion devices tested in Kanayama's study. (A) The BAK device, titanium threaded cage (D=13mm, L=20mm) (B) The BAK Proximity, titanium threaded cage (D=13mm, L=20mm) (C) The RAY TFC, titanium threaded cage (D=14mm, L=21mm) (D) The Danek TIBFD, stainless steel threaded cage (D=16mm, L=26mm) (E) The single oval Harms, titanium cylindrical mesh cage (17mm x 22mm x 13mm) (F) The double oval Harms, titanium cylindrical mesh cage (D=14mm, L=13mm) (G) The Brantigan PLIF, carbon fiber rectangular cage (13mm x 13mm x 24mm) (H) The Brantigan ALIF, carbon cylindrical rectangular cage (24mm x 35mm x 13mm) (I) The femoral ring allograft, sliced femoral shaft (20mm x 24mm x 14mm) (J) The bone dowel, dowel-shaped allograft with one hole (D=14mm, L=18mm) (K) The InFix device, titanium cylindrical implant (21mm x 29mm x 15mm) (from Kanayama et al., 2000, J Neurosurg (Spine 2))

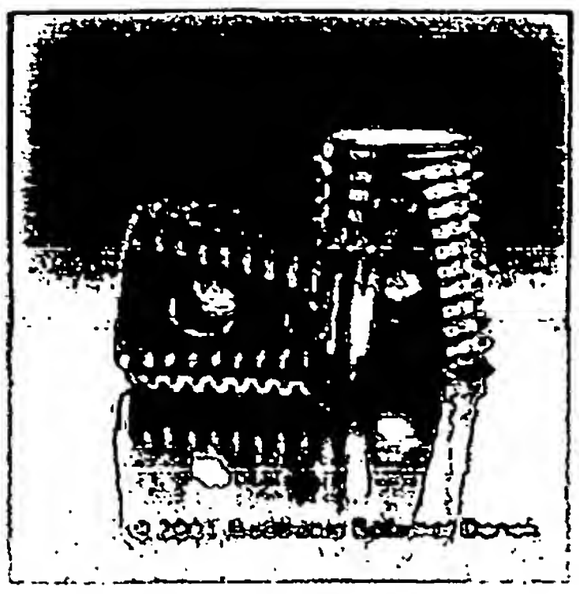

Figure 3 Wedged design of interbody fusion cages (LT-cage, Medtronic Sofamor Danek)

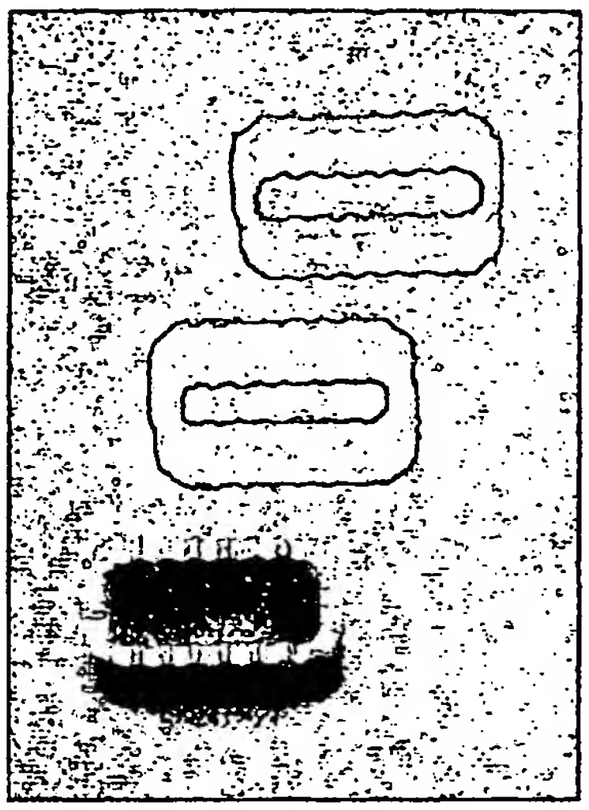

Figure 4 Poly-L-lactic acid (PLLA) interbody fusion cages. Vertical and rectangular configuration with the same diameter (10 x 10 x 18 mm). Top: flexible PLLA cage. Middle: stiff PLLA cage. Bottom: titanium cage. (from van Dijk et al., 2002, Spine)

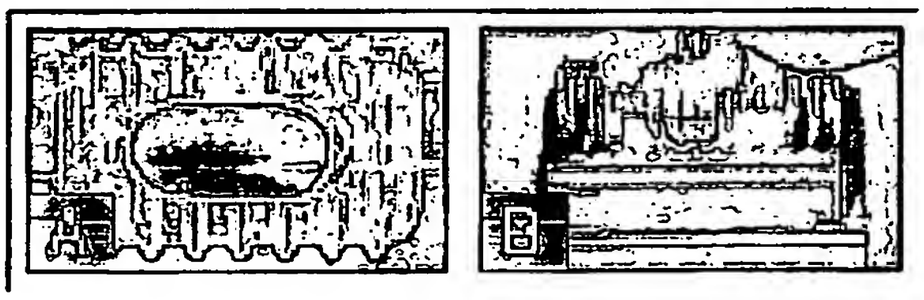

Figure 5 (A) 70/30 D,L-PLa interbody fusion device prior to implantation. (B) Iliac crest autograft or rhBMP-2 on a collagen sponge was packed into the thrugrowth slot of the device. (from Toth et al., 2002, Orthopedics)

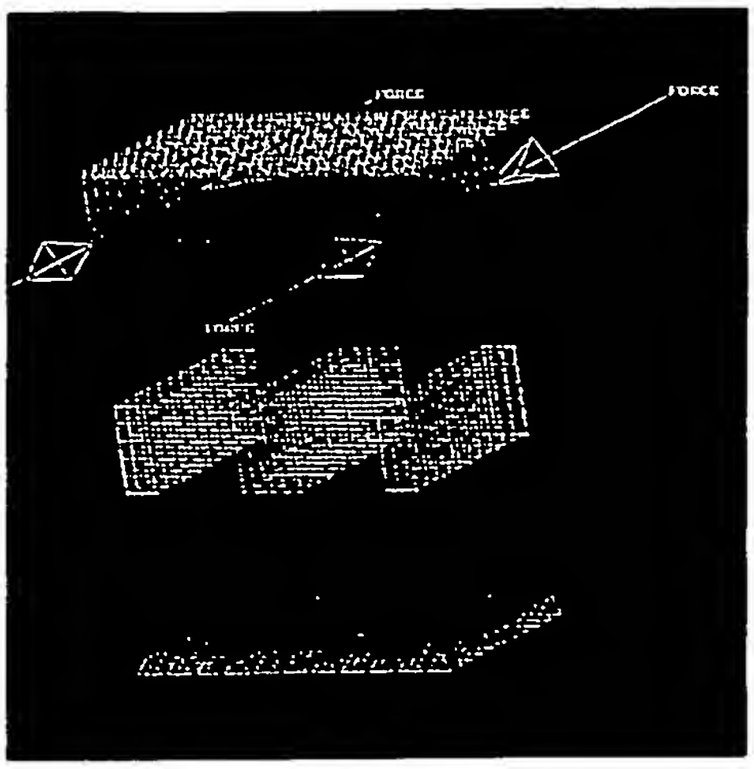

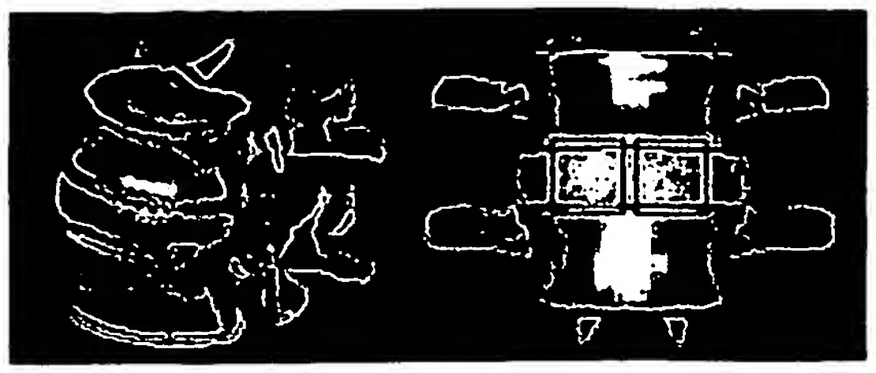

Figure 6L4-L5 segmental level of lumbar spine model to process topology optimization

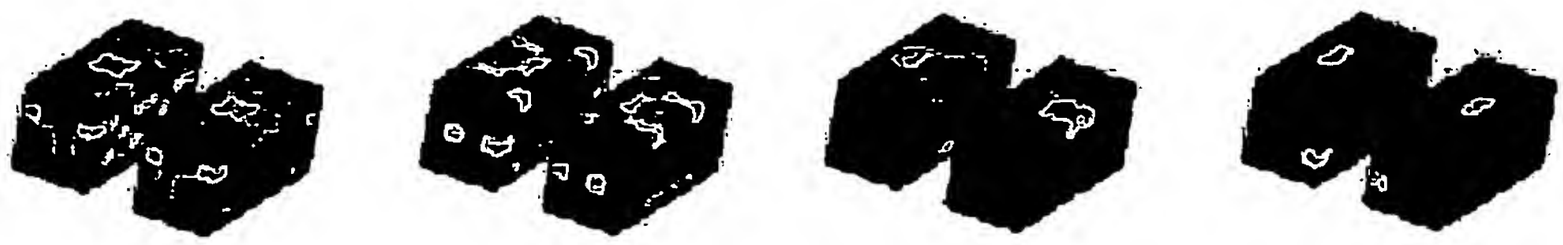

Figure 7Block configuration of density distributions at desired time points during degradation (based on poly(propylene fumarate)/beta tricalcium phosphate). (a) t=0T, E=1 GPa, (b) t=0.5T, E= 875 MPa, (c) t=0.55T, E=780 Mpa, and (d) t=0.85T, E=250 Mpa. (T: total degradation duration). Note that red color represents the most solid region, whereas the dark blue represents the most void, in between are intermediate material density.

a b c d

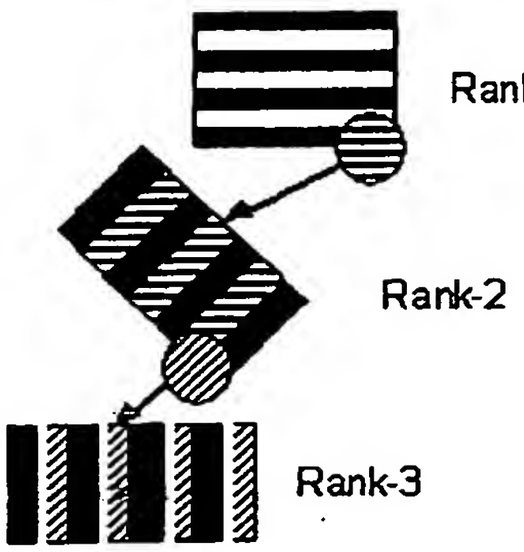

Figure 8

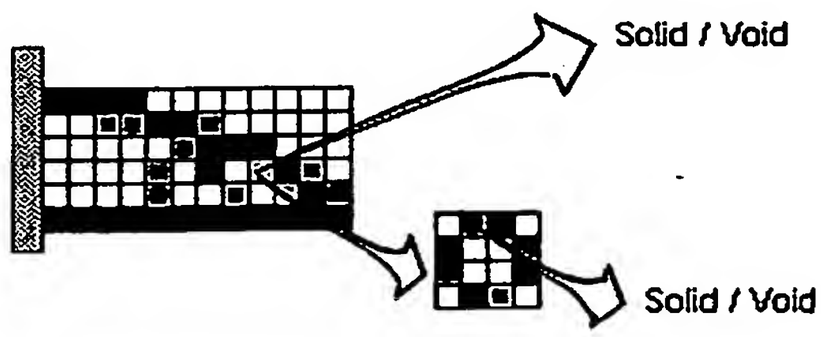

Figure 9

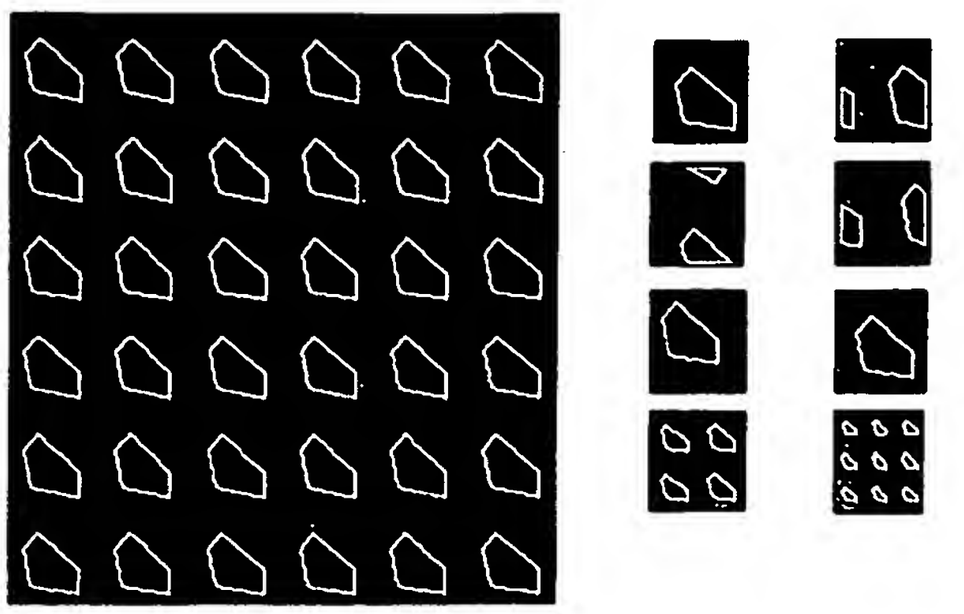

Figure 10

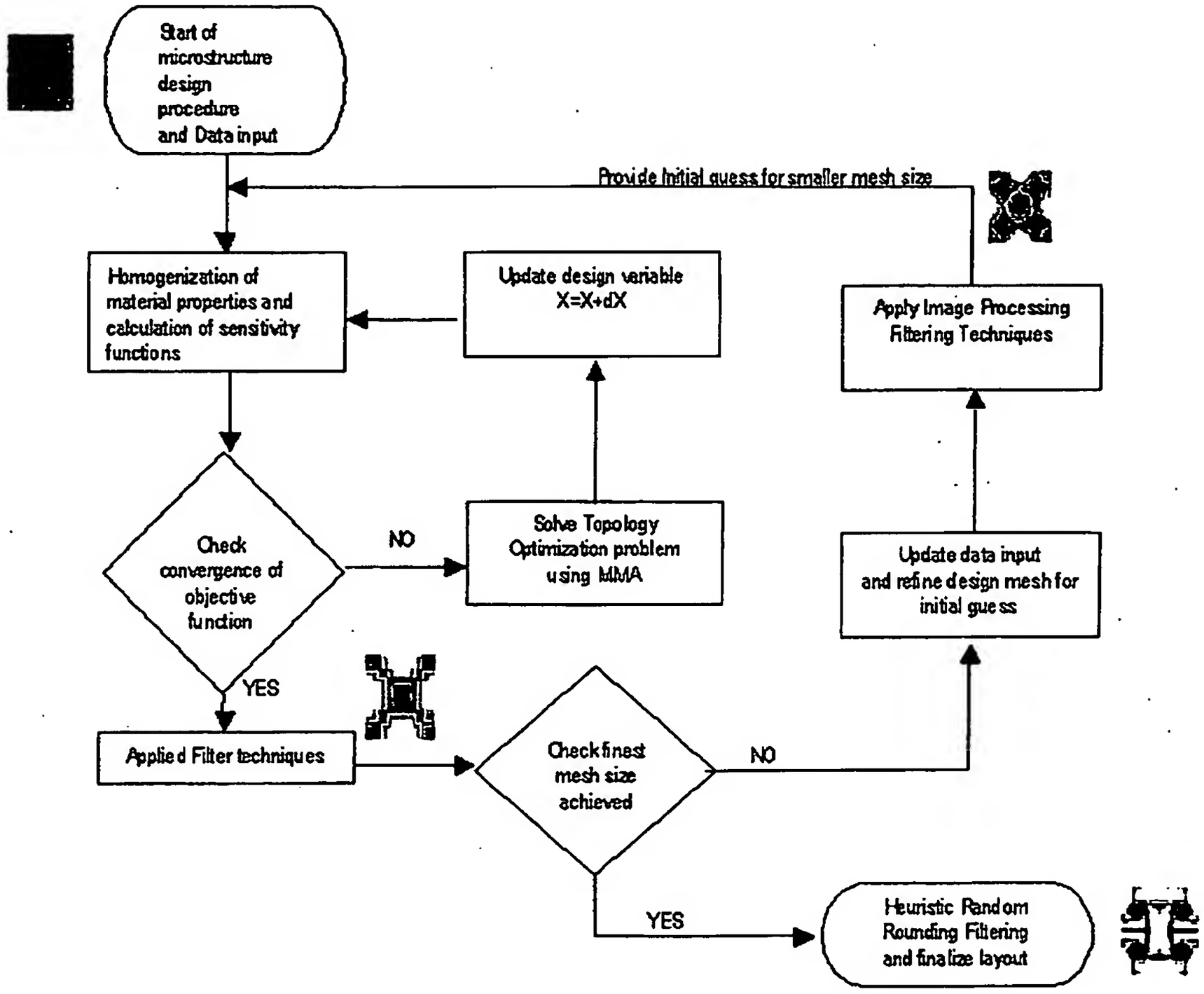

Figure 11

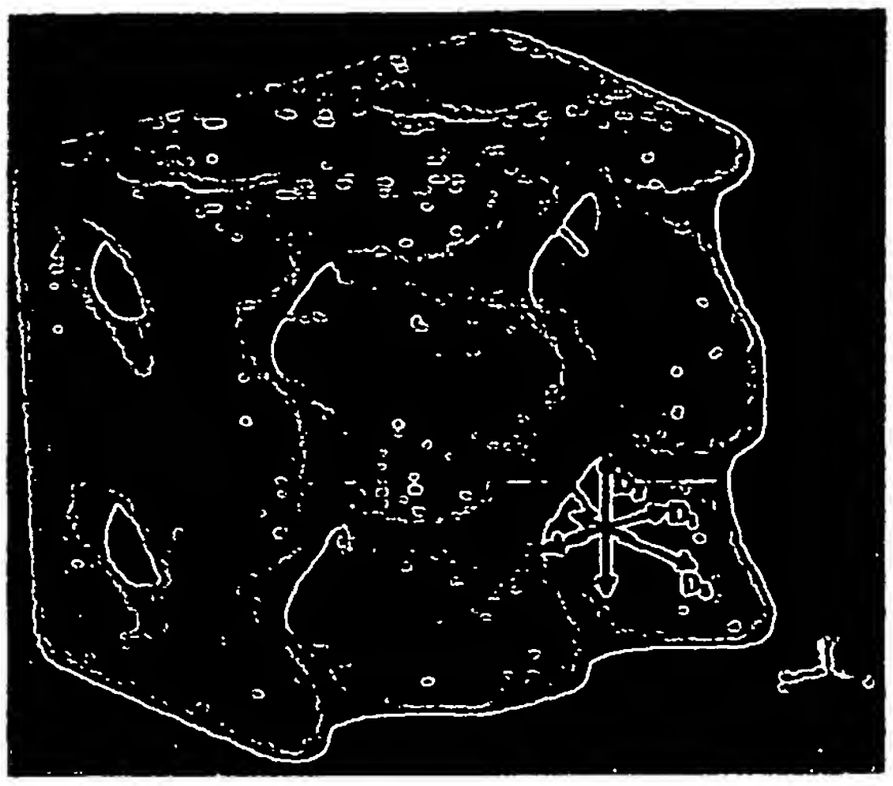

Figure 12 A cutaway showing the basic unit cell structure of interconnecting orthogonal cylinders. The pores are assumed to fill with regenerate tissue

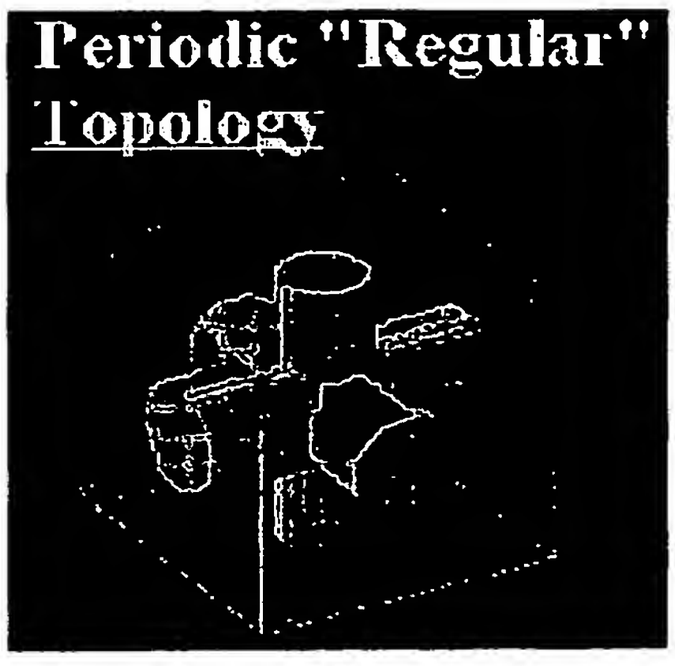

Figure 13 Topology of interconnecting cylinders constructing internal pore spaces

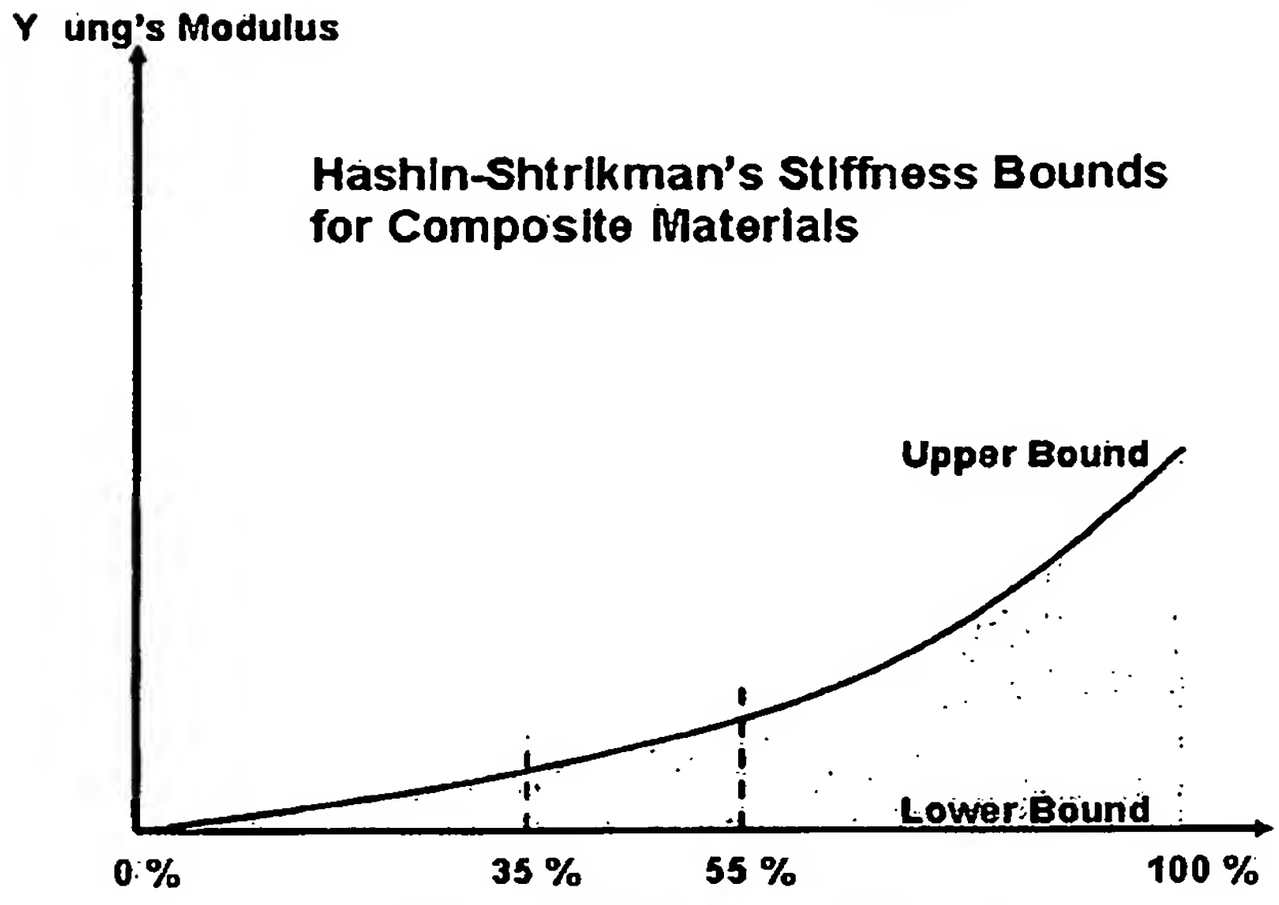

Figure 14 **Hashin-Shtrikman's stiffnes bounds**

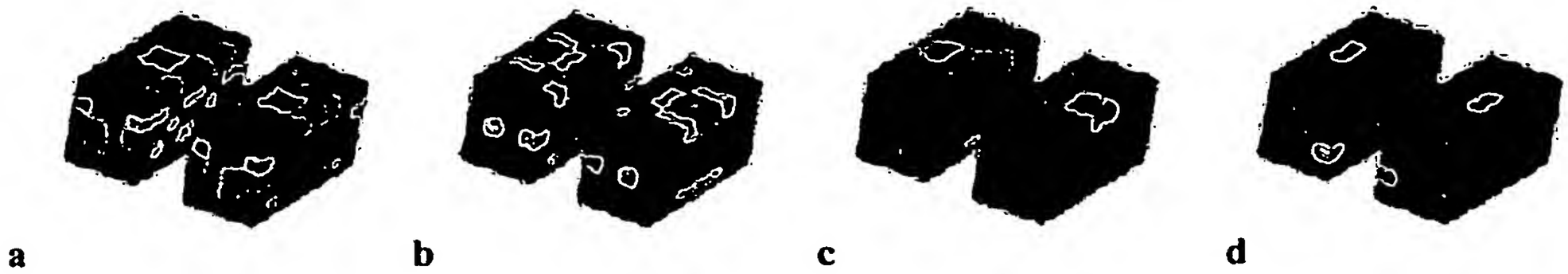

Figure 15 **Block configuration of density distributions at desired time points during degradation (based on poly(propylene fumarate)/beta tricalcium phosphate). (a) t=0T, E=1 GPa, (b) t=0.5T, E= 875 MPa, (c) t=0.55T, E=780 Mpa, and (d) t=0.85T, E=250 Mpa. (T: total degradation duration). Note that red color represents the most solid region, whereas the dark blue represents the most void, in between are intermediate material density.**

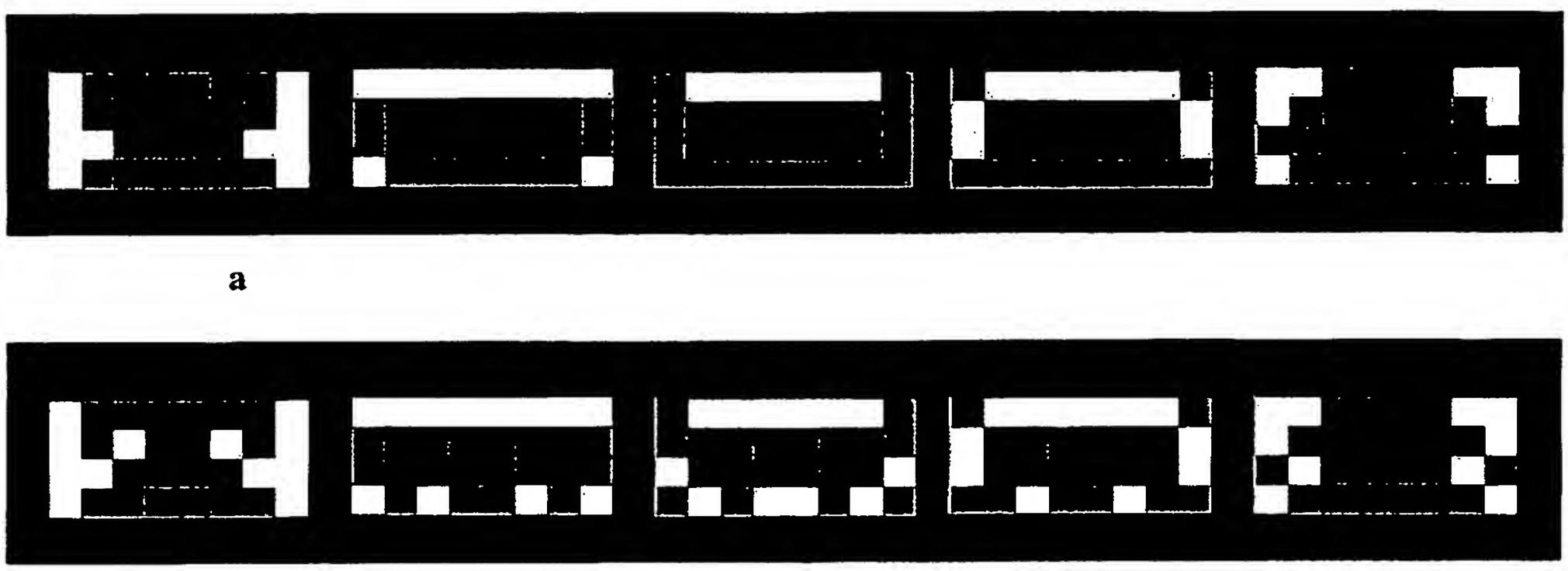

Figure 16 **Layout density segmented into four phases after threshold processing. Dark gray and light gray regions will later be replaced by corresponding microstructure of 55% and 35% volume fraction, respectively. (a) Layout density distribution on each layer of the spine cage design without material density weighting. (b) Layout density distribution on each layer of the spine cage design applying the material density weighting with consequent material density distributions of reduced base material stiffness**

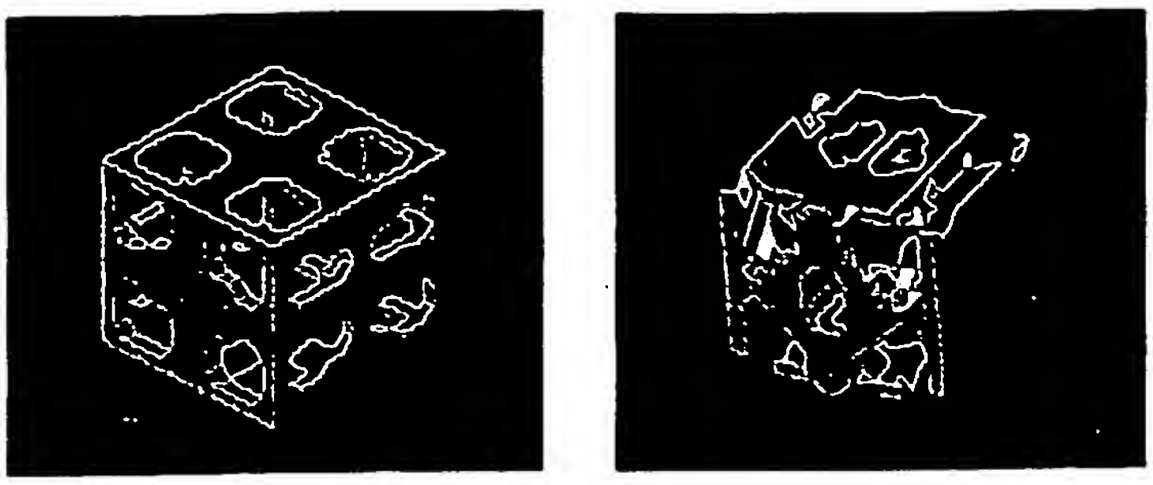

Figure 17 **Microstructure design of 35% volume fraction (left) and 55% (right)**

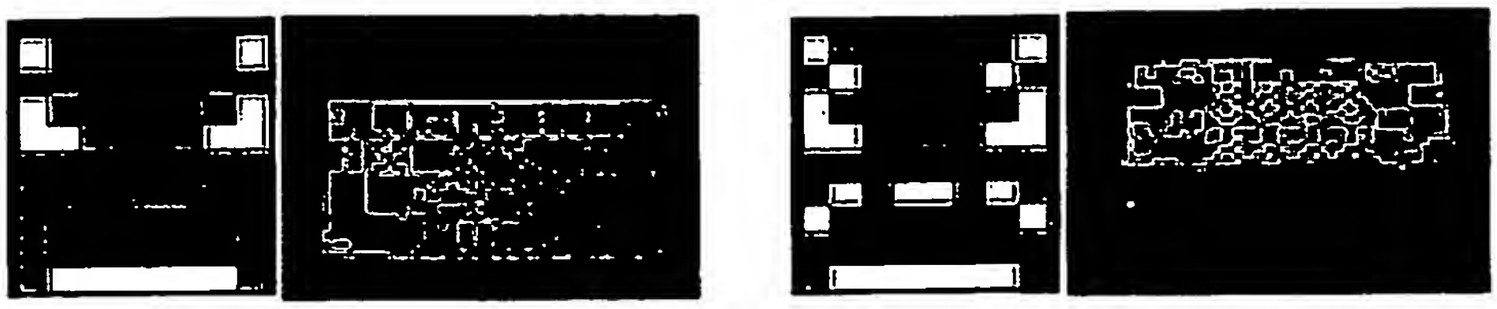

Figure 18 **Designed biodegradable PPF/β-TCP spine interbody fusion cages by the disclosed approach. Left: designed cage by integrated topology optimization method without material density weighting. Right: designed cage by integrated topology optimization method without material density weighting.**

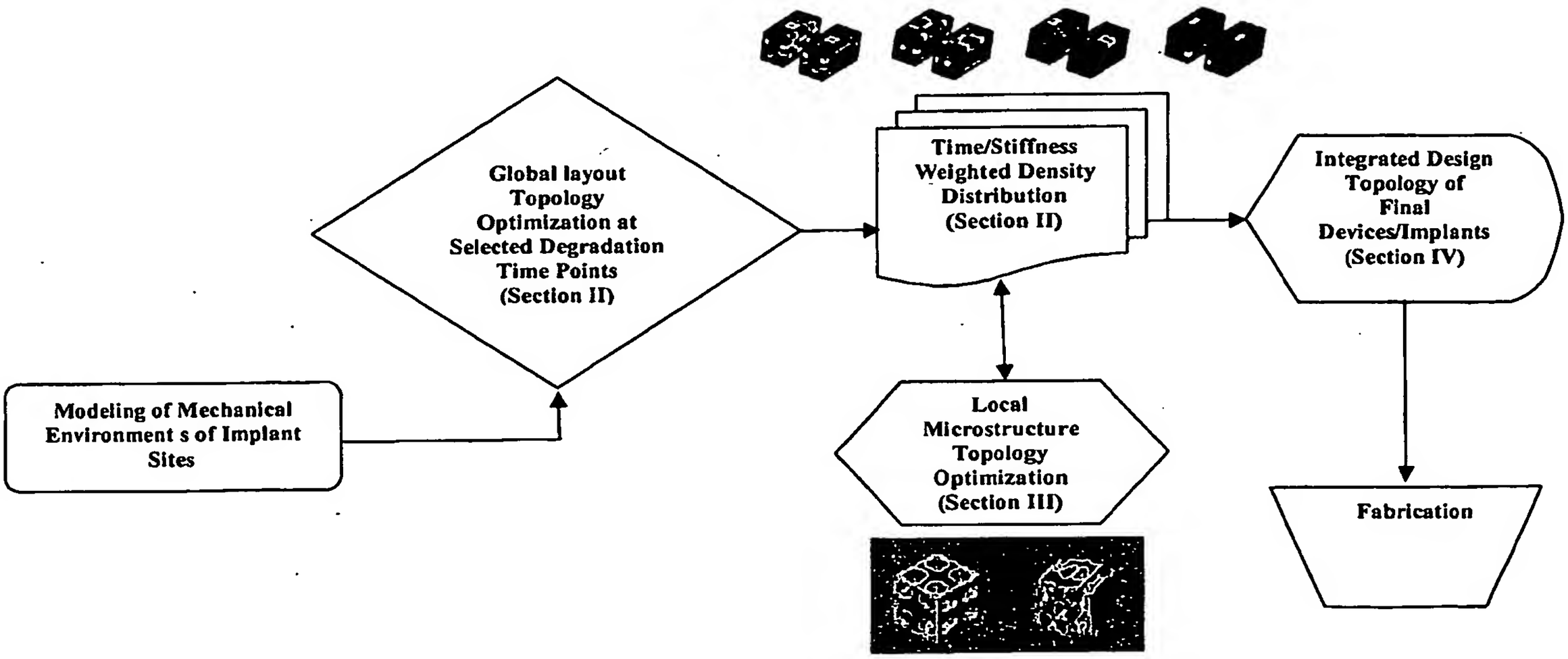

Fig. 19

INVENTOR INFORMATION

Inventor One Given Name:: Chia-Ying
Family Name:: Lin
Postal Address Line One:: 2131 Glencoe Hills Dr., Apt. 10
City:: Ann Arbor
State or Province:: Michigan
Country:: United States
Postal or Zip Code:: 48108
City of Residence:: Ann Arbor
State or Province of Residence:: Michigan
Country of Residence:: United States
Citizenship Country:: Taiwan
Inventor Two Given Name:: Scott
Family Name:: Hollister
Postal Address Line One:: 2105 Churchill Drive
City:: Ann Arbor
State or Province:: Michigan
Country:: United States
Postal or Zip Code:: 48103
City of Residence:: Ann Arbor
State or Province of Residence:: Michigan
Country of Residence:: United States
Citizenship Country:: United States

CORRESPONDENCE INFORMATION

Correspondence Customer Number:: 27572
Fax One:: 248 641 0270

APPLICATION INFORMATION

Title Line One:: BIODEGRADABLE/BIORESORBABLE TISSUE AUGME
Title Line Two:: NTATION/RECONSTRUCTION DEVICE
Total Drawing Sheets:: 8
Formal Drawings?:: No
Application Type:: Provisional
Docket Number:: 2115-002753
License US Govt. Agency:: National Institute of Health
Contract or Grant Numbers One:: DE13416, DE13608
Secrecy Order in Parent Appl.?:: No

Source:: PrintEFS Version 1.0.1

Document made available under the Patent Cooperation Treaty (PCT)

International application number: PCT/US04/040298

International filing date: 03 December 2004 (03.12.2004)

Document type: Certified copy of priority document

Document details: Country/Office: US
Number: 60/527,455
Filing date: 05 December 2003 (05.12.2003)

Date of receipt at the International Bureau: 31 January 2005 (31.01.2005)

Remark: Priority document submitted or transmitted to the International Bureau in compliance with Rule 17.1(a) or (b)

World Intellectual Property Organization (WIPO) - Geneva, Switzerland
Organisation Mondiale de la Propriété Intellectuelle (OMPI) - Genève, Suisse